Cyclization Kinetics of Nondiluted Bond Fluctuation Chains

Ana M. Rubio, Marcos Pita, and Juan J. Freire*

Departamento de Química Física, Facultad de Ciencias Químicas, Universidad Complutense, 28040 Madrid, Spain

Received December 18, 2001; Revised Manuscript Received April 15, 2002

ABSTRACT: A dynamic Monte Carlo algorithm has been employed to explore the cyclization of flexible linear chains without hydrodynamic interactions. The chains are represented by the bond fluctuation model in the semidilute and concentrated (or melt) regimes. We have obtained the decay rates of the cyclization process for different values of chain length, concentration, and capture radius of the reacting ends. In agreement with the theoretical predictions, the rate decays clearly show a short-time and a long-time behavior. The results are compared with quantitative theoretical results for both the short- and long-time regimes.

Introduction

Cyclization of flexible polymers is an interesting feature, which has important practical implications as this type of reaction may compete with chain growth in some types of polymerization. From the experimental point of view, it can also be associated with a variety of photophysical experiments.[1] We will focus on the formation of a loop by the irreversible reactive approach of the two ends of the chain at a distance closer than a given capture radius, which has been the object of a significant amount of theoretical and simulation analysis in the past. The problem is associated with basic concepts in the theoretical treatment of polymer systems as excluded-volume and hydrodynamics interactions. These two features should be considered for a realistic description of dilute polymers in a good solvent, but they are screened out for increasing polymer concentrations and can be ignored in the case of melts.

Years ago, Wilemski and Fixman[2] formulated the theoretical basis to this problem in the dilute regime. They used the Rouse−Zimm model[3] to describe the dynamics of the chains. Assuming a diffusion-controlled kinetics, they also employed a sink operator, describing the change of the distribution function by means of a closure approximation. The cyclization constant depends on the time correlation function of the end-to-end vector, which, according to the Rouse or Zimm theories, is mainly determined at long times by the first Rouse relaxation time of the chain, τ_1. It also depends on the ratio between the capture radius and the root-mean-squared end-to-end distance.

Other theoretical schemes describing the cyclization process in dilute and nondilute systems have been proposed later. De Gennes formulated a general approach to this purpose.[4] The application of reptation theory[3] to the case of cyclization in melts was developed later in detail by Noolandi et al.[5] and O'Shaughnessy.[6] Although the basic approximation of the Wilemski and Fixman theory, namely the calculation of the distribution function using a sink, is maintained, it is assumed that the sink has the form of a δ function (similarly to the description of intramolecular interactions in the excluded-volume theory). This leads to the prediction of cyclization constants that only depends on the mean relaxation time of the chains. This magnitude determines the meantime needed to have the two ends in contact, if they are previously apart from each other. Noolandi et al. were able to quantitatively predict the cyclization constants in the long-time and short-time limits for fully entangled systems. At long time, they simply obtained

$$k_c(t\rightarrow\infty) \equiv k_\infty = 0.895/\tau = 0.363/\tau_r \qquad (1)$$

while, at short time, their result was

$$k_c(t=0) \equiv k_0 = (0.655/\tau)(t/\tau)^{-1/4} = (0.333/\tau_r)(t/\tau_r)^{-1/4} \qquad (2)$$

where $\tau = (\pi^2/4)\tau_r$ and τ_r is the longitudinal or disengagement relaxation time of the chain, $\tau_r \approx N^3\Phi^{2(1-\nu)/(3\nu-1)}$ (N is the number of segments, Φ is the polymer volume fraction, and ν is a critical exponent, $\nu \approx 0.6$). τ_r also determines the long time relaxation of the end-to-end vector, and therefore, it is equivalent to the relaxation time of the first Rouse mode of the chain τ_1. (τ_1 can be numerically obtained in nonentangled or entangled conditions, independent of whether the Rouse dynamics applies or not.) The results at short times in this theory do not take into account cyclizations due to bead jumps inside the reptation tube.[3] These results were generalized by O'Shaughnessy,[6] studying the behavior at shorter times and considering also two other cyclization cases where inner units are involved. For the end-to-end cyclization this more recent theory predicts two additional short-time ranges, characterized by much smaller relaxation times, in which the ends move inside the reptation tube or just diffuse as individual segments within a smaller blob without interacting with other beads.

Friedman and O'Shaughnessy[7] have employed the scaling and renormalization group theory to obtain cyclization rates from "first principles", i.e., avoiding any approximation for the sink. They studied end-to-end and inner cyclizations. Their results describe several different situations for which entanglements are not important, providing scaling laws for dilute solutions and quantitative results for systems corresponding to the free-draining limit, i.e., in the absence of hydrodynamic interactions, case originally considered by Rouse.[3] Actually, the behavior of short-chain melts or for short enough time (more precisely, for cases where the dynamics is not affected by entanglements) may correspond to the case of free-draining systems without

10.1021/ma012205d CCC: $22.00
Published on Web 06/06/2002

excluded-volume effects. The theoretical prediction for this case gives expressions for the cyclization constant at short and long times that are in qualitative agreement with eqs 1 and 2. However, it yields a different front factor ($A_1 = 16/\pi^3 = 0.516$ for both time regimes). Different proportionality constants are obtained for other cases. For example, $B_1 = 8/\pi^3 = 0.258$ is found, also for both time regimes, when free-draining systems with excluded-volume effects are considered. Moreover, in the latter excluded-volume case, the exponent $-1/4$ in eq 2 must be substituted by -0.11. For free draining, the relaxation time should be consistent with Rouse dynamics,[3] i.e., with $\tau_1 \approx N^2$ (not excluded volume) or $\tau_1 \approx N^{2.18}$ (excluded volume).

A fundamental question, discussed through ref 7, is that the cyclization kinetic process cannot be always considered a diffusion-controlled process. On the contrary, it may obey the simpler "law of mass action" for some of the cases and, therefore, should be proportional to the equilibrium probability of finding the two ends at short distance, $k_c \approx W(R = 0)$, where $W(R)$ is the end-to-end distance equilibrium distribution function. For a long flexible polymer, this function depends on the scale variable $R/\langle R^2\rangle^{1/2}$ and the strength of excluded-volume conditions (which create a "correlation hole"[7] for the probability near to $R = 0$). Since excluded-volume effects are progressively screened out as polymer concentration increases above the overlapping value, Φ^*, changes in concentration or solvent quality have an important role in this limit not only by controlling the medium viscosity or friction but also through their varying influence on $W(R=0)$.

In fact, the scaling law dependence of the inverse Rouse relaxation times on chain length can be compared with the corresponding dependence of $W(R=0)$, leading to a basic prediction of the kinetic behavior.[7] It can be assumed that the proportionality constants in these scaling laws are not very different for the two possibilities. Consequently, it is reasonable to assign the kinetics control to the regime whose associated magnitude, $1/\tau_1$ or $W(R=0)$, decreases more rapidly with N, which implies a much smaller rate constant for long chains. This way, it is shown that the cases obeying the law of mass action mainly correspond to the dilute regime in good solvents, where both hydrodynamic interactions and excluded-volume effects are present. Most systems that do not show these effects are predicted to show diffusion control. Consistently, this is the case of melts, since τ_1 has a strong dependence on N, while the non-excluded-volume distribution function $W(R=0)$ is greater and decreases more slowly with N. The explicit influence of $W(R=0)$, $\langle R^2\rangle$, and R_0 on the cyclization rates is canceled in the diffusion-controlled cases. This was shown in refs 5 and 6 for the case of chains obeying reptation theory. However, diffusion control may not hold in the earliest time regimes,[6] where dynamics is inside the tube and it is not longer governed by τ_R.

Some numerical simulations have also been aimed to study cyclization dynamics. Brownian dynamics simulations of single chains, with or without consideration of excluded-volume or hydrodynamic interactions, have been performed in previous work involving one of the present authors.[8−10] The numerical results were compared with the version of the Wilemski and Fixman theory reformulated for finite chains by Perico and Cuniberti.[11] A detailed comparison of the results from the most extended trajectories with the renormalization group theory results[12] showed that, in fact, the cases for which the law of mass action applies correspond to those predicted according to the scaling theory. This comparison with renormalization theory also serves to determine the value of the capture radius of the discrete chain simulation model that best reproduces the theory prediction. (In addition to the incorporation or not of excluded-volume and hydrodynamic interactions, this study included also two additional types of internal cyclizations, involving an end and an inner beads, or two inner beads, which were compared with the theoretical predictions of ref 7.) Moreover, the influence of the impenetrability of chains has been specifically studied in other Brownian dynamics simulations (without including hydrodynamic interactions).[13]

For nondilute solutions, the overall motion of the chain is affected by the system entanglements. Consequently, τ_1 increases with N significantly faster than is predicted by the Rouse theory.[3,14] For fully entangled chains, $\tau_1 = \tau_r$. Moreover, it can also be expected that the short-time regime can be more easily distinguished. (The Wilemski and Fixman theory[2] predicted that the cyclization decays are more than 99.9% single exponentials in the dilute regime, and this result has been confirmed by the simulation data;[8−10] therefore, the analysis of the short-time behavior was not possible for these systems.)

In the present work, we use a dynamic Monte Carlo algorithm to simulate cyclization of linear chains in different nondilute systems. We consider different values for chain length, concentration, and capture radius and compare the numerical results with the theoretical predictions in the short- and long-time regimes. The dynamic Monte Carlo allows for the generation of "Monte Carlo trajectories" in which the time variable is measured in units of Monte Carlo steps. A Monte Carlo step engulfs the number of stochastic changes of configuration necessary to ensure a single move opportunity for each one of the chain beads in the system.

If we want to mimic the real coarse-grained dynamics of polymer chains, it is necessary than the Monte Carlo algorithm only contemplates local stochastic changes or bead jumps.[15] For this reason, we represent the polymer chains as self-avoiding walk (SAW) chains, placed in a simple cubic lattice according to the bond fluctuation model specifications.[16,17] The bead jumps are particularly random and simple for this model, and it is generally believed[16] that they can provide a good representation of the chain dynamics. It should be mentioned that the Monte Carlo algorithms cannot easily incorporate hydrodynamic interactions. Nevertheless, the temporary formation of entanglements and the chain impenetrability are realistic physical features reproduced by the bond fluctuation model. Therefore, it is useful to study semidilute or concentrated solutions for which the hydrodynamic interactions are effectively canceled.[3,14] (For these systems explicitly dynamic algorithms are impractical or extremely costly, from the computational point of view.) Some of the concentrated solutions of bond fluctuation model chains can also actually describe the melt properties. In fact, it has been shown that systems with sufficiently long chains show results compatible with the reptation theory,[18] though we are not using such long chains in the present study. We will rather focus in the study of shorter chains, some of them well above overlapping concentration, for which the departure from Rouse dynamics due to entangle-

ment effects should be clearly observed, though some of the most subtle features related with reptation may not appear. We should mention that an off-lattice bead-jump algorithm has been recently employed to describe the cyclization dynamics of single chains with charged reactive groups.[19]

Several conformational and dynamic magnitudes (particularly chain sizes and the relaxation times of several Rouse modes) have been previously obtained for the same systems considered here.[20] The relaxation times of the first Rouse mode, which are relevant for the analysis of results in this work, were reported in Table 6 of ref 20. The overlapping concentrations for each chain length can be obtained as[14,20]

$$\Phi^* \cong 8N/(4\pi\langle S^2\rangle_0^{3/2}/3) \tag{3}$$

where $\langle S^2\rangle_0$ is the mean-squared radius of gyration of single chains (dilute solution). For the present chain lengths, they range from 0.036 to 0.078.[20]

Computational Methods

Generation of Trajectories. The algorithm details are described in refs 20 and 21. According to the model specifications, we put n chains, each composed of N beads in a cubic lattice of length L, with periodic boundary conditions. The distance between adjacent sites, b, is taken as the length unit. SAW conditions are adequately enforced so that two beads cannot be at a distance smaller than 2. The value of L is chosen high enough so that the number of interactions between different replicas of the same chain is very small.[22] A set of different chain lengths is considered in the model, with root-mean quadratic value $l = 2.72$. The number of chains is determined from the desired number of sites blocked by polymer beads, equivalent to the polymer volume fraction, $\Phi = 8nN/L^3$. (This definition justifies eq 3.)

Elementary bead jumps are achieved just by randomly moving a bead to one of the six adjacent sites. Time is assumed to the number of attempted moves or Monte Carlo steps. A step engulfs nN attempted moves and defines our time unit. The dynamic trajectories are run starting with previously equilibrated configurations. Typical trajectories consist of 4×10^6–2×10^7 Monte Carlo steps.

Cyclization Decays. The cyclization decay function $\varphi(t)$ gives the fraction of chains whose ends have not yet reacted, i.e., have not reached a distance within the capture radius, expressed as R_0 (also in units relative to b) at the given time. It can be simply related with the apparent cyclization constants included in theoretical expressions as eqs 1 and 2 through

$$\varphi(t) \approx \mathrm{e}^{-k_c t} \tag{4}$$

by adequately fitting the simulation data for short or long times.

To obtain $\varphi(t)$, we have analyzed the trajectory for different values of t, starting at a given configuration at $t = 0$, where the chains are defined to be open. A variable $n(t)$, used as a counter, is set to the value $n(t=0) = n$. For values of $t > 0$, we check the distance between the ends in all the chains open at the previous step. Every time one of these distances is smaller than the capture radius, we subtract one to the counter and the chain is marked as cycled, and it is not considered at further checks. (However, the resulting loop is not topologically enforced in subsequent simulation steps.) The checks are performed using the trajectory coordinates outside the box in order to avoid "false cyclizations" due to interactions between images of the same chain inside the box. (Even though the box size is high enough to reproduce most equilibrium and dynamic properties, this "false cyclizations" may represent 10–50% of the small total number of detected cyclizations inside the box.) After a given configuration has been checked this way, the probability associated with this configuration is simply obtained as $\varphi(t) = n(t)/n$. In most cases, it is not necessary to check all configurations in the trajectory, but only configurations taken every 20, 40, or 80 Monte Carlo steps. We have verified that, for typical cases, the decay curves obtained this way are very similar to those calculated by considering all the steps. However, to get good statistics, we have used four trajectories generated from different random number seeds. The final results for $\varphi(t)$ correspond to the arithmetic means obtained at each given time with the four independent samples.

As described in the Introduction, the equilibrium distribution function $W(R=0)$ may determine in some cases the cyclization dynamics. Therefore, we have also estimated this magnitude from the trajectories. Our evaluation is performed by counting the number of "closed" chains on 10^3 noncorrelated configurations along the trajectories. With this end, we use the same set of values of R_0 employed in the determination of k_c. $W(R=0) \cong W(R<R_0)$ is therefore determined from the total number of closed chains in each case. The final value is normalized accordingly with volume, number of chains, and number of checked configurations.

Table 1. Equilibrium Cyclization Probabilities Estimated for Different Values of the Capture Radius

		W(R=0)			
N	Φ	$R_0 = 2$	$R_0 = 3$	$R_0 = 4$	$R_0 = 5$
40	0.075	2.4×10^{-6}	8.8×10^{-6}	1.0×10^{-5}	1.1×10^{-5}
40	0.15	4.1×10^{-6}	1.5×10^{-5}	1.5×10^{-5}	1.6×10^{-5}
40	0.3	6.2×10^{-6}	2.3×10^{-5}	2.2×10^{-5}	2.4×10^{-5}
40	0.50	1.2×10^{-5}	3.1×10^{-5}	3.1×10^{-5}	3.2×10^{-5}
100	0.075	$\cong 10^{-7}$	1.7×10^{-6}	2.1×10^{-6}	2.1×10^{-6}
100	0.15	$\cong 10^{-7}$	2.6×10^{-6}	3.0×10^{-6}	3.8×10^{-6}
100	0.3	1.0×10^{-6}	5.6×10^{-6}	6.0×10^{-6}	6.1×10^{-6}
100	0.5	2.7×10^{-6}	8×10^{-6}	7×10^{-6}	8×10^{-6}

Results and Discussion

The results for $W(R<R_0)$ are contained in Table 1 for our shorter and longer chains at different concentrations. The results for $R_0 = 2$ are very small and suffer larger statistical oscillations, since only a few cycled chains can be detected in the chosen sample. The beads cannot actually be at distances smaller than 2. Moreover, at this minimum distance, the correlation hole effect due to excluded-volume effects is important for the most diluted systems.[7] As will be shown below, this small value of the capture radius gives the best description of the cyclization processes, which will be under diffusion control. The values of $W(0)$ are greater for higher capture ratios for which the dependence on capture radius is weak. (The covered range of the reduced variable $R/\langle R^2\rangle^{1/2}$ is narrow, and therefore, the equilibrium distribution functions cannot vary much; even if the correlation hole is present, $W(0)$ is closer to its maximum.) For $R_0 > 2$, $W(R<R_0)$ increases monotonically with concentration (due to the progressive screen-

ing of the excluded-volume effects, which shrinks the chains) and decreases with chain length. In the most diluted systems, the latter decrease is significantly more pronounced than the expected $N^{-3/2}$ dependence for a Gaussian chain, also due to the excluded-volume effects.

Figure 1 show the logarithmic plots of the calculated cyclization decays for the longest chain length, $N = 100$, and different values of the capture radius, R_0, at different concentrations. A noticeable curvature is observed in the short-time regime. This curvature becomes more significant as the concentration of the system increases. At any rate, a well-defined linear long-time behavior can be defined in all cases. The cyclization constant k_∞ can, therefore, be easily obtained in this regime. The constants show a log−log linear dependence vs chain length, and it is observed that the slopes in these plots for different systems do not significantly depend on the capture radius. Moreover, they are similar (with opposite signs) to those calculated for the chain length dependence of the first Rouse mode in our previous investigation of the same systems.[20] In fact, linear fits of the cyclization constants vs the values of $1/\tau_1$ obtained for the systems yield good correlations and small ordinates (see Figure 2); i.e., they are consistent with

$$k_c = C/\tau_1 \qquad (5)$$

in good qualitative agreement with eq 1 (assuming $\tau_r = \tau_1$). However, the slopes of the latter fits, C, are not constant. Figure 3 contains the results for the apparent proportionality constants vs concentration. (As can be expected, the slopes increase significantly with the capture radius.)

On the other hand, the Friedman et al. theory[7] predicts the proportionality constant of $A_1 = 0.516$ for chains that obey Rouse dynamics without excluded volume (in first order of the perturbation variable $\epsilon = 4 - d$, where $d = 3$ is the space dimension). This result was found compatible with the data obtained with this conditions from Brownian dynamics simulations of single chains.[12] These simulations were performed with chain lengths similar to those used in the present study but employing an off-lattice model.[8−10] Important variations with the capture radius were also observed. Assuming that the most adequate value of R_0 for the model is obtained by comparing the simulation proportionality constant with the theoretical prediction, the best agreement was found with $R_0/l \cong 0.5$. Our results for $R_0 = 2$, or $R_0/l \leq 0.73$, are also in reasonable quantitative agreement with A_1 for the range of concentration $\Phi = 0.075-0.15$. The values of C are constant or suffer a moderate decrease in this range of concentration. These concentrations can be considered to correspond to semidilute solutions, according to our previous analysis of the collective scattering functions for the same systems.[21] Therefore, it seems that the Rouse dynamics gives a reasonable reproduction of the end-to-end cyclization corresponding to our semidilute solutions at long times. It should be considered that the chains are relatively short and the Rouse dynamics may prevail even above overlapping concentration. However, we believe that semidilute solutions of longer chains are considerably more entangled and may not obey Rouse dynamics.

Furthermore, a strong dependence of $W(R=0)$ on N, as the one shown in Table 1 for the most diluted systems, may indicate significant excluded-volume effects. The analysis of the variation of the mean size data with chain length, performed in previous work,[20] also

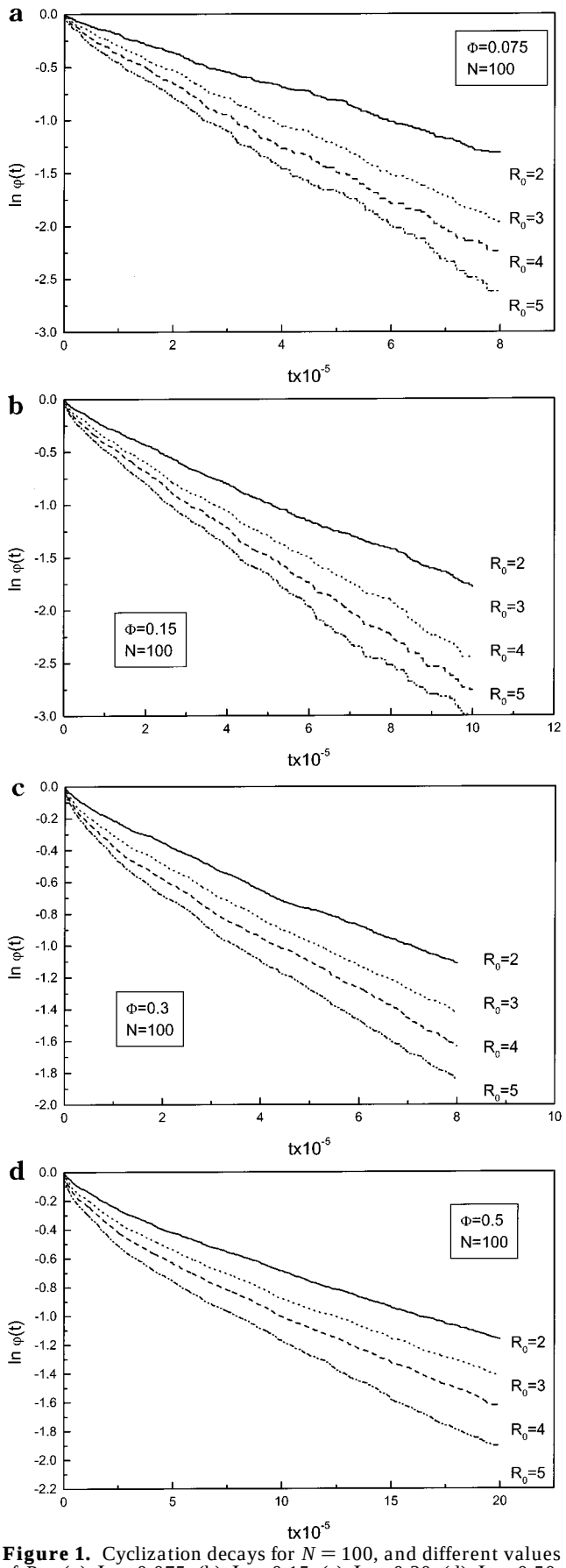

Figure 1. Cyclization decays for $N = 100$, and different values of R_0: (a) $\Phi = 0.075$; (b) $\Phi = 0.15$; (c) $\Phi = 0.30$; (d) $\Phi = 0.50$.

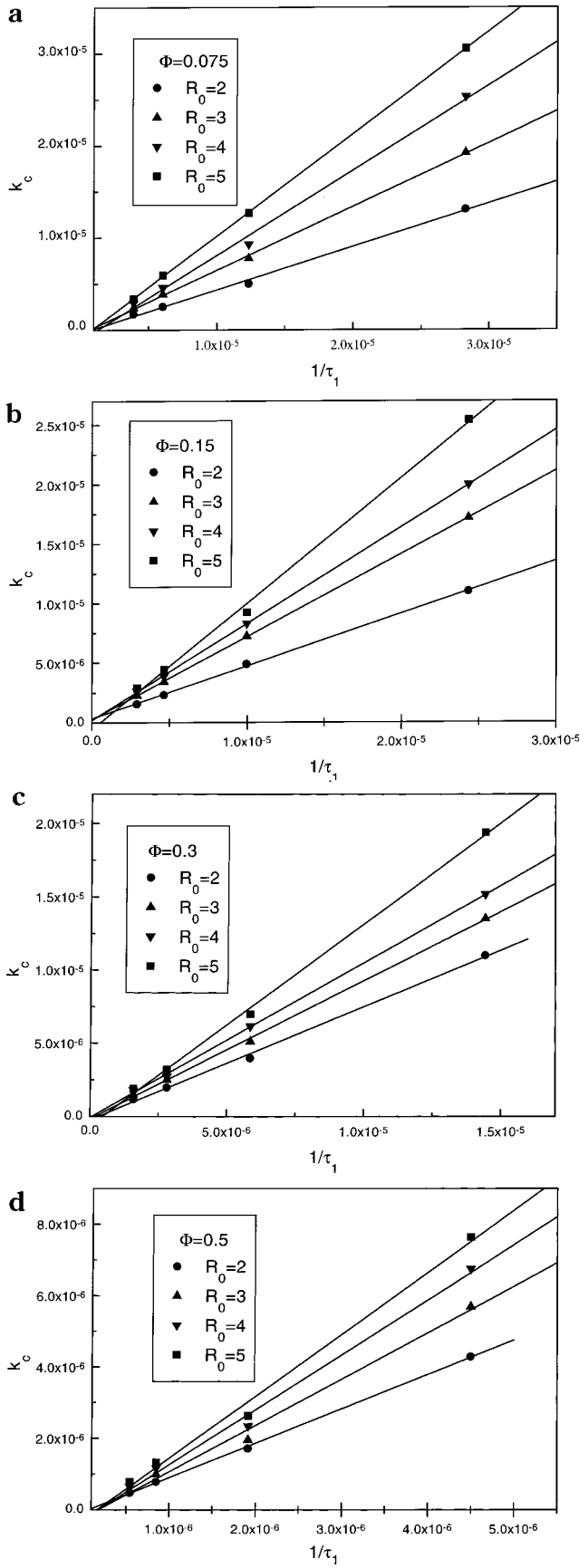

Figure 2. Long-time cyclization constants vs $1/\tau_1$ and different values of R_0: $R_0 = 2$, circles; $R_0 = 3$, up triangles; $R_0 = 4$, down triangles; $R_0 = 5$, squares. (a) $\Phi = 0.075$; (b) $\Phi = 0.15$; (c) $\Phi = 0.30$; (d) $\Phi = 0.50$.

supports this conclusion, which is also suggested by the analysis of the short-times data, as we will explain

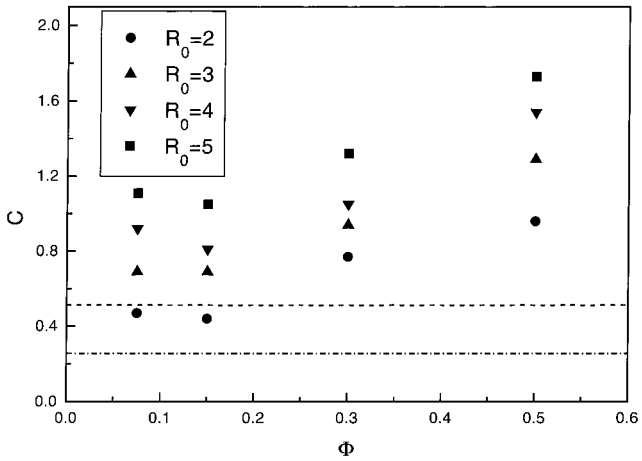

Figure 3. Proportionality constants, C (from the linear fits of k_c obtained at long times, vs $1/\tau_1$, shown in Figure 2, according to eq 5), vs concentration for different values of R_0. Dash line: renormalization group theory constant for free draining case without excluded volume, A_1. Dash and dot line: renormalization group theory constant for free draining case with excluded volume, B_1.

below. Assuming Rouse dynamics with full excluded-volume effects, the renormalization group theory predicts a common short-time and long-time coefficient $B_1 = A_1/2$ (also in first order). Our numerical results of C for $R_0 = 2$ are too large compared with this prediction. We have incorporated constant B_1 to be compared with the C values in Figure 3. It can be observed that the data for the two smallest concentrations lie between A_1 and B_1. The particular choice of the capture radius for our discrete chain simulation model surely affects this comparison. Since $R_0/l = 0.5$ seems to be the best choice for dilute systems, at least for the Brownian dynamics off-lattice model,[12] it is reasonable to assume that our data for $R_0 = 2$ may be higher than the optimum value. In fact, the variation of the proportionality constant with the capture radius observed in Figure 3 suggests that a value of the capture radius closer to $R_0/l = 0.5$ would yield data for our dilute systems consistent with the first-order coefficient prediction for excluded-volume systems, B_1. However, this smaller value of R_0 cannot be investigated with for our lattice model.

The slopes C show a clear increase with concentration for the other two values of Φ, which correspond to concentrated systems, with any value of the capture radius. The data with $R_0 = 2$ yield a proportionality constant of about 0.9 at high concentrations ($\Phi = 0.5$ can, actually, represent the case of a melt[23]). It is not clear whether this result should give an upper limit for real systems, or C should increase with concentration to reach even larger values for chains long enough to obey the tube model. (Our chains may be considered short to agree with the reptation theory even at high concentrations. However, we believe that they are long enough to be free of the finite chain effects predicted for $N < 30$ with a free-space "chain-of-links" model.[24]) In any case, assuming that the reptation time can be identified with our numerical values of τ_1, our values of C for the more entangled systems (and with the smallest capture radius) are about 3 times higher than the proportionality constant of eq 1. The factor can be reduced to 2 assuming a hypothetical smaller capture radius, as suggested in the preceding paragraph. It is therefore shown that, contrary to the quantitative theoretical prediction, the increase of friction due to

entanglement formation at high concentration has a stronger influence on the relaxation times than on the cyclization constants. In other words, the simulations indicate that the prefactors are significantly higher than those predicted from first principles for systems in which the Rouse theory prevails (A_1 or B_1). According to more recent theoretical considerations,[6] however, the closure approximation is unreliable for the quantitative calculation of cyclization constants, where the sink term is always apparently a large perturbation of the equilibrium distribution.

In previous work,[10] we have provided numerical estimations of this effect, by comparing our Brownian dynamics simulation data for single chains with numerical values obtained from the Wilemski and Fixman theory. Although both sets of results depend on the capture radius value and chain length, the ratios between them were found to be practically constant. In the absence of excluded-volume and hydrodynamic interactions, the simulation data are about twice the theoretical values. The theoretical treatment leading to eq 2 considers entanglements and describes the sink through a δ function, as basic differences with respect to the Wilemski and Fixman theory. However, if we admit that the main source of disagreement of this treatment with our simulation data for the most concentrated systems is the approximate introduction of the sink, it is not surprising that we find a similar factor of 2 in the present case.

The short-time regime is characterized by the curvature clearly shown in Figure 1. To investigate this behavior, the apparent single-exponential rates consistent with eq 4 at short t have to be subsequently fitted to a power law that can be maintained for a relatively wide interval of time values. Therefore, we have fitted the short-time simulation data of $\varphi(t)$ to

$$\ln[-\ln \varphi(t)]_{t\cong 0} = \ln c + a_0 \ln t \qquad (6)$$

which agrees with eq 2 for $a_0 = {}^3/_4$, $\tau = \tau_1$, $k_0 = ct^{(a_0-1)}$, and

$$c = C_0/\tau_1^{a_0} \qquad (7)$$

where C_0 should correspond to the numerical proportionality constant in eq 2, the qualitatively equivalent renormalization group prediction based on the Rouse model (which also yields constant $A_1 = 0.512$ in the short-time regime) or any other similar theoretical form related with relaxation time τ_1. The fits are generally good, expanding over most of the time simulation time range (typically $t > 10^3$). Therefore, we assign these fits to the first short-time regime prevailing at times below τ_1. At smaller times, we found different behaviors strongly dependent on the particular system considered in each case. Thus, in some of the systems, we observe an initial increase (with exponent close to 1) apparently followed by a flatter increase or a plateau. It could be tempting to assign these regions to the regimes theoretically predicted at short times.[6] In other systems, the plateau is somehow extended to the shortest times, with very small cyclization number of reacted chains, suggesting that these data are "law of mass action" controlled ($W(R{=}0)$ is very small in most systems, as observed in Table 1). It is simpler and more reasonable, however, to interpret this features as "steps" due to the significant statistical noise inherent to our numerical procedure to determine k_c in this range of very short times. Therefore, we have mainly focused our attention in the interpretation of the final and more extended short-time regime, well described by the fits.

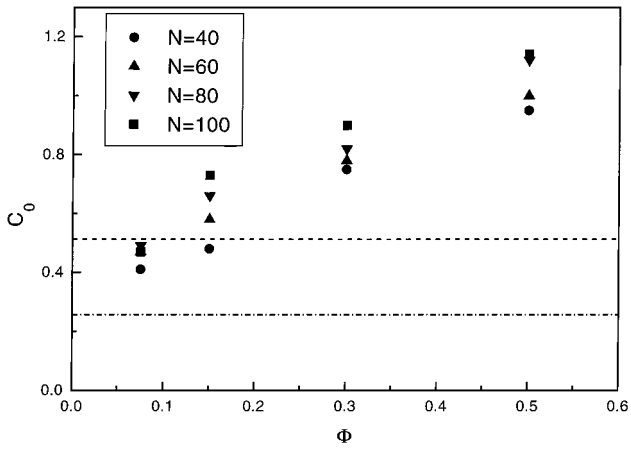

Figure 4. Proportionality constants, C_0 (from the linear fits of the cyclization times at shorter times to eqs 6 and 7), vs concentration obtained with $R_0 = 2$ and different values of N. Dash line: renormalization group theory constant for free draining case without excluded volume, A_1. Dash and dot line: renormalization group theory constant for free draining case with excluded volume, B_1.

The fitted values of a_0 do not change systematically with the chain length, except for the $\Phi = 0.15$ case, which will be detailed below. However, the results have a systematic decrease for increasing values of the capture radius R_0. For the highest concentrations, the results are close to the theoretical prediction, $a_0 = {}^3/_4$, only for $R_0 = 2$. Maintaining this capture radius value fixed, we observe a small but systematic decrease of a_0 for increasing concentrations. For $R_0 = 2$, $a_0 \cong 0.8{-}0.9$ for the most diluted chains. This can be explained by the increasing excluded-volume effects in these systems, which are closer to overlapping concentration, since the theoretical value of this exponent for systems with excluded volume obeying Rouse dynamics[7] is $a_0 \cong 1{-}0.11 = 0.89$. All this seems again to indicate that $R_0/l < 1$ is the best option for the capture radius.

We should also note that the short-time fits are similarly adequate (with the same fitting parameters) to describe the time range $t \cong \tau_1$. This is a general feature, even though the data in this range also exhibit a constant value of C when the data are linearly fitted (with good correlation) in ln k_c vs t plots, as described above. For the longer chains, eq 6 finally yield $a_0 \cong 1$ only for values of t greater than $\tau = 2.47\tau_1$. Therefore, $\tau \geq t \geq \tau_1$ seems to be a crossover connecting the short-time and long-time regimes. This region is characterized by a progressive but smooth increase of a_0.

The fitted values of c and the previously obtained results for τ_1 were introduced in eq 7 to calculate C_0. We will limit our discussion to the results obtained with for $R_0 = 2$. These results, shown in Figure 4, should be compared with those obtained for the long time proportionality constant C. The values of C_0 for the shortest chain, $N = 40$, are practically identical to C at any concentration. For longer chains, however, C_0/C increases and have a value of about 1.20 for the longest chains and most concentrated systems. These ratios, however, do not show a systematic dependence on concentration, having a maximum for $\Phi = 0.15$. Nevertheless, eq 1 and the renormalization group theory for free-draining dynamics (both with and without

excluded volume) predict $C_0/C \cong 1$. It can be noted from eqs 5−7 that a larger value of the ratio C_0/C implies a higher value of t for which the short-time and long-time equations give the same k_c. Therefore, the crossover between these two regimes, discussed in the preceding paragraph, is somehow extended from τ_r to τ for the longer chains. Constant C_0 increases strongly in the concentrated systems, consistent with the similar behavior observed for C.

The differences between C and C_0 may be related with the nonexponential behavior observed for the Rouse modes in entangled systems.[20,25] The end-to-end vector relaxation function (directly related with cyclization) shows a curvature with faster initial relaxation with respect to the predictions of the Rouse or the tube theory.[26,27] (Both theories lead to a common formally equivalent expression for this function, in terms of τ_1.) This effect suggest a faster effective relaxation at short times, consistent with the higher proportionality constants found when our numerical estimations of τ_1 are introduced to estimate the cyclization constants.

Also with this assumption, we can mainly interpret the increase of C_0 for the longer chains at $\Phi = 0.15$ as the manifestation of the onset of entanglement regime, due to the increase of Φ/Φ^*. ($\Phi = 0.15$ is, in fact, the concentration where a larger a variation of a_0 is found, from 0.9 for $N = 40$ to 0.8 for $N = 100$. Moreover, the mean size dependence on chain length for this concentration shows a behavior intermediate between those expected for systems with or without excluded-volume effects.[20]) It is not clear, however, why this increase is only manifested in the short-time regime. (The values of C at the same concentration do not exhibit any clear N dependence.) It is possible that the long time regime well above overlapping concentration explores large regions where the local excluded-volume variation is not relevant. However, the short-time regime may explore regions of sizes comparable to the system blobs. At lower concentrations, the Rouse dynamics with excluded volume prevails in both times regimes, while at higher concentration blobs are considerable smaller, and we observe the effect of entanglements at short and long times.

We can conclude that our simulations are able to characterize a long-time and a short-time behavior for the cyclization constants of chains in systems with concentrations ranging from overlapping conditions to melts. Both regimes are related with the chain's main relaxation time and qualitatively consistent with the theoretical expectations. For our most diluted systems, we find proportionality constants compatible with the renormalization group theory applied for the case of Rouse dynamics with or without excluded-volume conditions, considering the influence of the capture radius choice on the cyclization values and the low order perturbation of the theoretical predictions. At higher concentrations, or more entangled systems, predictions from a "first principles" theory are not available and results have to be compared with a theoretical prediction based on the reptation theory with a sink closure approximation. The cyclization rates decrease more slowly than expected from the theory, which may not be quantitatively reliable.

Acknowledgment. This work has been supported by Grant PB98-0791 from the "Dirección General de Enseñanza Superior e Investigación Científica" (DGESIT), Ministerio de Educación y Cultura, Spain. Our previous characterization of the bond fluctuation model was performed within the TMR European Network Project "NEWRUP". J.J.F. carried out the final steps of the manuscript preparation at the "Departamento de Ciencias y Técnicas Experimentales, Universidad Nacional de Educación a Distancia", Madrid, Spain.

References and Notes

(1) *Cyclic Polymers*; Semlyen, J. A., Ed.; Elsevier: New York, 1986.
(2) Wilemski, G.; Fixman, M. *J. Chem. Phys.* **1974**, *60*, 866, 878.
(3) Doi, M.; Edwards, S. *The Theory of Polymer Dynamics*; Clarendon: Oxford, 1986.
(4) De Gennes, P.-G. *J. Chem. Phys.* **1982**, *76*, 3316.
(5) Noolandi, J.; Hong, K. M.; Bernard, D. A. *Macromolecules* **1984**, *17*, 2895.
(6) O'Shaughnessy, B. *J. Chem. Phys.* **1991**, *94*, 4042.
(7) Friedman, B.; O'Shaughnessy, B. *Macromolecules* **1993**, *26*, 4888.
(8) García Fernández, J. L.; Rey, A.; Freire, J. J.; Fernández de Piérola, I. *Macromolecules* **1990**, *23*, 2057.
(9) Rey, A.; Freire, J. J. *Macromolecules* **1991**, *24*, 4673.
(10) Ortiz-Repiso, M.; Rey, A.; Freire, J. J. *Macromolecules* **1998**, *31*, 8356.
(11) Perico, A.; Cuniberti, C. *J. Polym. Sci., Phys. Ed.* **1977**, *15*, 1435.
(12) Ortiz-Repiso, M.; Rey, A. *Macromolecules* **1998**, *31*, 8356.
(13) Podtelezhnikov, A.; Vologodskii, A. *Macromolecules* **1997**, *30*, 6668.
(14) de Gennes, P.-G. *Scaling Concepts in Polymer Physics*; Cornell: Ithaca, NY, 1979.
(15) Boots, H.; Deutch, J. M. *J. Chem. Phys.* **1977**, *67*, 4608.
(16) *Monte Carlo and Molecular Dynamics Simulations in Polymer Science*; Binder, K., Ed.; Oxford University Press: New York, 1995.
(17) Carmesin, I.; Kremer, K. *Macromolecules* **1988**, *21*, 2819.
(18) Paul, W.; Binder, K.; Heerman, D. W.; Kremer, K. *J. Chem. Phys.* **1991**, *95*, 7726.
(19) Stampe, J.; Sokolov, I. M. *J. Chem. Phys.* **2001**, *114*, 5043.
(20) Rubio, A. M.; Storey, M.; Lodge, J. F. M.; Freire, J. J. *Macromol. Theor. Simul.* **2002**, *11*, 171.
(21) Rubio, A. M.; Lodge, J. F. M.; Freire, J. J. *Macromolecules*, in press.
(22) Kremer, K. *Macromolecules* **1983**, *16*, 1632.
(23) Wittmer, J.; Paul, W.; Binder, K. *Macromolecules* **1992**, *25*, 7211.
(24) Bernand, D. A.; Noolandi, J. *J. Math. Phys.* **1984**, *25*, 1619.
(25) Shaffer, J. S. *J. Chem. Phys.* **1995**, *103*, 761.
(26) Freire, J. J.; Adachi, K. *Macromolecules* **1995**, *28*, 4747.
(27) Kaznessis, Y. N.; Hill, D. A.; Maginn, E. J. *J. Chem. Phys.* **1998**, *109*, 5078.

MA012205D